8.A.8 Nuclear Physics B17 (1970) 168-188. North-Holland Publ. Comp., Amsterdam

SCATTERING OF NEGATIVE PIONS ON CARBON

F. BINON *++, P. DUTEIL *, J. P. GARRON ‡, J. GORRES ‡‡,
L. HUGON **, J. P. PEIGNEUX **, C. SCHMIT ‡,
M. SPIGHEL *‡ and J. P. STROOT *‡+

CERN-IPN (Orsay) Collaboration
CERN, Geneva, Switzerland

Received 1 December 1969

Abstract: Data are presented on elastic and inelastic differential cross sections as well as on total cross sections for negative pions on carbon in the energy range 120 MeV to 280 MeV.

1. INTRODUCTION

The aim of this experiment was to study elastic and inelastic pion-nucleus scattering at incident pion energies around the first $(\frac{3}{2}, \frac{3}{2})$ pion-nucleon resonance, in order to: (i) gain knowledge on how pions interact with nuclei when the pion-nucleon interaction is strongly dominated by a resonance; (ii) deduce selection rules and probabilities of excitation of nuclear levels in the presence of such a resonance.

The status of these problems was rather poor: (i) there were no experimental data available in this energy range; (ii) there still is no firmly established theoretical approach; the Kisslinger and Ericson model is successful for energies below 100 MeV, and the Glauber model works only for pion energies larger than $\approx$ 500 MeV.

In order to achieve the proposed programme it was necessary to make improvements to the experimental technique so as to: (i) obtain high momentum resolution for the separation of individual nuclear levels; (ii) build a variable-energy pion beam with sufficiently high intensity between 100 MeV and 300 MeV.

* CERN, Geneva, Switzerland.
** Faculté des sciences de Clermont-Ferrand, France.
‡ IPN, Faculté des sciences, Orsay, France.
‡‡ Kernforschungszentrum und Universität, Karlsruhe, Germany.
+ IISN, Brussels, Belgium.
++ FNRS, Brussels, Belgium.

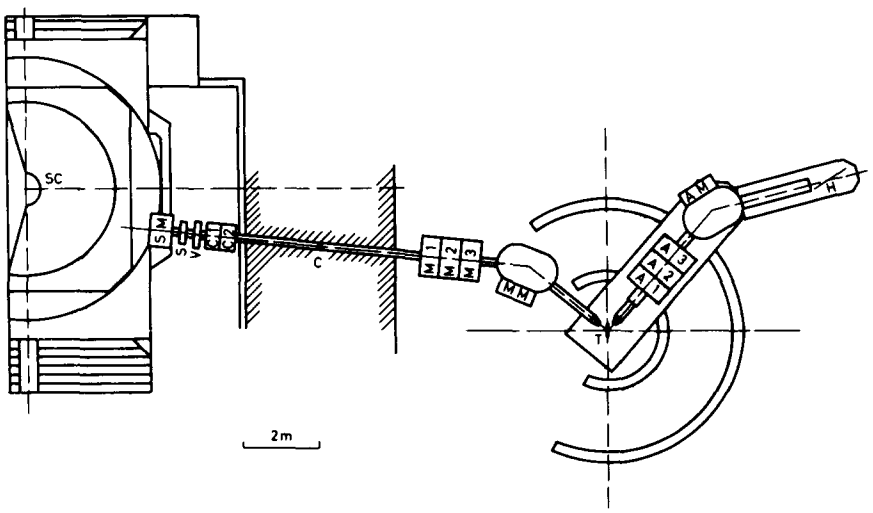

Fig. 1. General layout of the experiment. Variable energy beam: SM - steering magnet, S - sextupole, V - vertical deflector, C1-C2 - quadrupole lenses, C - collimator. Monochromator: M1-M2-M3 - triplet of quadrupole lenses, MM - 35^o bending magnet. T - target. Analyser: A1-A2-A3 - triplet of quadrupole lenses, AM - 35^o bending magnet. H - hodoscope.

2. EXPERIMENTAL METHOD

The fig. 1 shows the general layout of the experiment at the CERN Synchro-cyclotron. Pions are produced on an internal Be target and are focused by a quadrupole doublet and the main SC magnet fringing field onto a collimator placed inside the SC shielding wall. The proper choice of the azimuthal position of the internal target and of the field in a special steering magnet, located between the SC coils very near to the main vacuum chamber, allows one to collect the negative pions produced in the forward direction with respect to the circulating proton beam for energies between 100 MeV and 300 MeV. A sextupole lens gives some correction to the higher-order aberrations.

The pions then enter a double achromatic spectrometer consisting of two very similar arms, one being the monochromator, the other being the analyser. Each consists of a symmetric triplet of quadrupole lenses and a 35^o bending magnet. Their horizontal magnification is about one. The analyser can be rotated up to an angle of 150^o to the monochromator beam line, but for practical reasons one could not measure at scattering angles larger than 140^o.

The scattering target is placed at the focus of the monochromator, where a dispersed horizontal image of the collimator is formed. At the target the momentum bite is about 2%, the beam angular dispersion is $\pm 2^o$ in both horizontal and vertical directions, and the beam intensity is $1.5 \cdot 10^5$ sec^{-1} at 180 MeV for a collimator opening of 8 mm horizontally

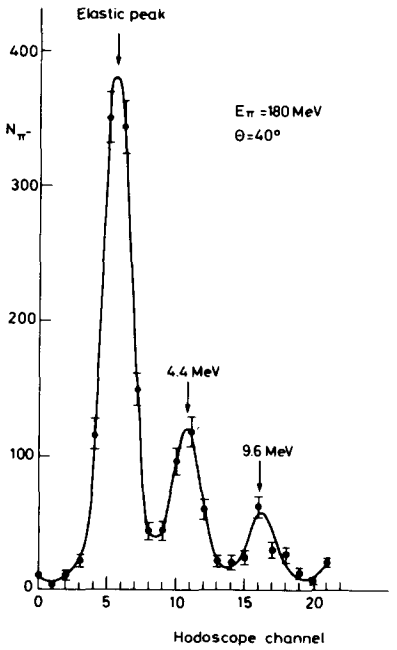

Fig. 2. Typical spectrum obtained with a 1 cm thick graphite target for incident pions of 180 MeV and for $\theta = 40^{\circ}$.

and 16 mm vertically. It drops to $5 \cdot 10^4$ sec^{-1} at 100 MeV and 300 MeV. Most measurements were made with 0.5 cm thick graphite targets of measured density. The particles which do not suffer any inelastic interaction in the target are refocused by the analyser, irrespective of their initial momentum because of the exact compensation of the dispersions in the two arms of the spectrometer. However, any pion which loses energy in the target is displaced along the analyser focal line by an amount fixed by the dispersion (1.5 cm for $\Delta p/p = 1\%$) of this arm alone. It thus allows the use of the full momentum bite in the incident beam without loss of resolution. The analyser acceptance is $(3.81 \pm 0.07) \cdot 10^{-3}$ sr.

A hodoscope of 23 scintillation counters, each 5 mm wide, is aligned along the focal line of the analyser. Small scintillation counters 0.5 mm thick, placed around the target, monitor the beam intensity and reduce the background. The over-all momentum resolution at the final hodoscope was $\Delta p/p \approx 0.5$ to 1%. It was not the ultimate resolution of the apparatus but it was quite sufficient to separate clearly the elastic peak from the 4.4 MeV level of carbon, as shown in fig. 2. This is a novel feature of this experiment.

3. ELASTIC SCATTERING

Angular distributions were measured between 10° and 140° at 120, 150,

180 and 200 MeV, and between 10^o and 70^o at 230, 260 and 280 MeV.

Corrections have been made for the measured counter efficiencies (> 90%), and for the decay of the pions between the carbon target and the final hodoscope. The latter effect ranges from 28% at 280 MeV to 45% at 120 MeV. The proportions of μ^- and e^- in the beam have been measured. Their contributions to the cross sections (maximum 3.4% at 10^o and 120 MeV) have been subtracted. The results, taking into account all the above-mentioned corrections, are given in the c.m. system in column 2 of table 1.

The combined finite angular resolution of the two parts of the spectrometer, including the effect of multiple scattering in the target, has been measured by observing the angular distribution around 0^o scattering angle. The angular width $\sqrt{\langle\theta^2\rangle}$ is 1.6^o. Correction has been made for this effect; its value is given in column 3 of table 1. Its influence is most important in the region of the first minimum, especially at 50^o in the 180 MeV data. The results, after this correction has been applied, are given in column 4 of table 1.

The finite momentum bandwidth of the beam (5 to 10 MeV/c, depending on the momentum) has not been taken into account. Its effect would be to fill in the dip at the diffraction minima very slightly.

The errors given in columns 2 and 4 of table 1 are the sum of the statistical error and of the error in the measured background. The uncertainties on the experimental parameters, including those coming from the above mentioned corrections, give an additional total error of scale which is given below columns 2 and 4 in table 1.

Possible systematic effects, such as those due to shifts in electronics, beam set-up, and SC conditions between runs, have been investigated by observing the variations of the pion elastic differential cross section as a function of energy at a series of $|t|$ values smaller than 20 000 $(\mathrm{MeV}/c)^2$.

Some deviations from a smoothly varying curve are larger than the estimated errors. A scaling factor has been obtained in trying to fit the angular distribution data together with the total cross section data ‡ (essentially free of systematic errors) with an optical potential model. It brings back the deviation inside the experimental errors. This factor seems to be a fair estimate of the systematical effects. Its value (table 2) is very close to one, except at 280 MeV, a fact which is not understood. The last column of table 1 gives the final result for the differential cross section, including the scaling factor. These results are presented in fig. 3, where $d\sigma/dt = (\pi/p^{*2})(d\sigma/d\Omega)^*$ has been plotted versus t. The lines drawn on the figures are guides to the eye and not the results of fits.

4. INELASTIC SCATTERING AND TOTAL CROSS SECTIONS

Together with the elastic cross sections, inelastic cross sections corresponding to excitation of individual nuclear levels or groups of levels in ^{12}C were also measured since (a) the useful range of excitation covered at

‡ See sect. 4.

Table 1
$\pi^- {}^{12}C$ differential elastic cross section.

Pion kinetic energy in the lab. system = 120 MeV				
Momentum in c.m. system = 213.92 MeV/c				
1	2	3	4	5
θ^* (deg)	$\left(\frac{d\sigma}{d\Omega}\right)^*$ (mb/sr)	finite angle correction	$\left(\frac{d\sigma}{d\Omega}\right)_\pi^{*FA}$ (mb/sr)	$\left(\frac{d\sigma}{d\Omega}\right)^{*SF}$ (mb/sr)
10.84	398.1 ± 19.8	0	398.1 ± 19.8	414.0 ± 20.6
11.87	348.6 ± 22.3	0	348.6 ± 22.3	362.5 ± 23.2
12.89	326.6 ± 19.0	0	326.6 ± 19.0	339.7 ± 19.8
13.91	314.3 ± 17.0	0	314.3 ± 17.0	326.9 ± 17.7
14.94	292.2 ± 12.2	0	292.2 ± 12.2	303.9 ± 12.7
15.97	258.5 ± 10.7	0	258.5 ± 10.7	268.8 ± 11.1
18.53	237.9 ± 8.6	0	237.9 ± 8.6	247.4 ± 8.9
21.07	200.8 ± 6.9	+0.2	201.0 ± 6.9	209.0 ± 7.2
26.16	138.5 ± 3.5	-0.2	138.3 ± 3.5	143.8 ± 3.6
31.27	89.6 ± 2.5	-0.4	89.9 ± 2.5	92.7 ± 2.6
36.38	60.0 ± 2.1	-0.5	59.5 ± 2.1	61.8 ± 2.2
41.56	29.0 ± 1.9	-0.4	28.6 ± 1.9	29.7 ± 2.0
46.64	12.4 ± 1.2	-0.3	12.1 ± 1.2	12.6 ± 1.2
51.72	6.07 ± 0.6	-0.2	5.87 ± 0.6	6.1 ± 0.6
56.79	3.26 ± 0.4	-0.1	3.16 ± 0.4	3.3 ± 0.4
61.85	1.97 ± 0.35	-0.04	1.93 ± 0.35	2.01 ± 0.36
66.90	1.50 ± 0.30	-0.01	1.49 ± 0.30	1.55 ± 0.31
71.94	1.75 ± 0.30	0	1.75 ± 0.30	1.8 ± 0.3
76.97	1.55 ± 0.30	0	1.55 ± 0.30	1.6 ± 0.3
87.01	0.75 ± 0.20	0	0.75 ± 0.20	0.78 ± 0.2
97.00	0.31 ± 0.14	0	0.31 ± 0.14	0.32 ± 0.15
111.93	0.083 ± 0.059	-0.002	0.081 ± 0.059	0.084 ± 0.061
131.69	0.60 ± 0.15	0	0.60 ± 0.15	0.62 ± 0.16
141.53	0.66 ± 0.15	0	0.66 ± 0.15	0.69 ± 0.16
	±5%		±5%	±6%
total error of scale				

Table 1 (continued)

Pion kinetic energy in the lab. system = 150 MeV

Momentum in c.m. system = 247.38 MeV/c

1	2	3	4	5
θ^* (deg)	$\left(\frac{d\sigma}{d\Omega}\right)^*$ (mb/sr)	finite angle correction	$\left(\frac{d\sigma}{d\Omega}\right)^{*FA}$ (mb/sr)	$\left(\frac{d\sigma}{d\Omega}\right)^{*SF}$ (mb/sr)
10.16	475.9 ±28.6	0	475.9 ±28.6	447.3 ±26.9
11.18	430.8 ±19.7	0	430.8 ±19.7	405.0 ±18.5
12.71	409.5 ±16.2	0	409.5 ±16.2	384.9 ±15.2
15.27	365.5 ±13.5	-1.5	364.0 ±13.5	342.1 ±12.7
20.40	264.4 ± 6.2	-1.5	262.9 ± 6.2	247.2 ± 5.8
25.62	169.9 ± 3.1	-1.2	168.7 ± 3.1	158.6 ± 2.9
30.73	98.1 ± 2.1	-1.0	97.1 ± 2.1	91.3 ± 2.0
35.84	50.3 ± 1.0	-0.7	49.6 ± 1.0	46.6 ± 0.9
40.94	22.9 ± 0.7	-0.5	22.4 ± 0.7	21.0 ± 0.7
46.04	8.3 ± 0.3	-0.4	7.9 ± 0.3	7.4 ± 0.3
51.12	2.56± 0.14	-0.18	2.38± 0.14	2.24± 0.13
56.20	1.18± 0.10	-0.07	1.11± 0.10	1.04± 0.09
58.73	0.70± 0.17	-0.07	0.63± 0.17	0.59± 0.16
61.27	1.02± 0.09	-0.03	0.99± 0.09	0.93± 0.08
66.32	1.48± 0.10	+0.01	1.49± 0.10	1.40± 0.09
71.37	1.27± 0.10	+0.01	1.28± 0.10	1.20± 0.09
76.41	1.22± 0.08	0	1.22± 0.08	1.15± 0.08
81.44	0.73± 0.06	0	0.73± 0.06	0.69± 0.06
86.45	0.40± 0.05	-0.01	0.39± 0.05	0.37± 0.05
91.46	0.15± 0.04	-0.01	0.14± 0.04	0.13± 0.04
96.45	0.11± 0.03	0	0.11± 0.03	0.10± 0.03
101.43	0.13± 0.03	0	0.13± 0.03	0.12± 0.03
111.36	0.32± 0.04	0	0.32± 0.04	0.30± 0.04
121.25	0.43± 0.06	0	0.43± 0.06	0.40± 0.06
140.93	0.23± 0.05	0	0.23± 0.05	0.22± 0.05
	±4%		±4%	±6%

total error of scale

Table 1 (continued)

Pion kinetic energy in the lab. system = 180 MeV

Momentum in c.m. system = 279.57 MeV/c

1	2	3	4	5
θ^* (deg)	$\left(\frac{d\sigma}{d\Omega}\right)^*$ (mb/sr)	finite angle correction	$\left(\frac{d\sigma}{d\Omega}\right)^{*FA}$ (mb/sr)	$\left(\frac{d\sigma}{d\Omega}\right)^{*SF}$ (mb/sr)
10.18	462.2 ± 29.4	0	462.2 ± 29.4	462.2 ± 29.4
11.21	454.7 ± 19.0	0	454.7 ± 19.0	454.7 ± 19.0
12.75	397.1 ± 15.0	0	397.1 ± 15.0	397.1 ± 15.0
15.32	362.0 ± 11.1	0	362.0 ± 11.1	362.0 ± 11.1
17.89	313.7 ± 7.0	0	313.7 ± 7.0	313.7 ± 7.0
20.46	242.1 ± 3.7	-0.5	241.6 ± 3.7	241.6 ± 3.7
25.57	147.8 ± 2.9	-1.0	146.8 ± 2.9	146.8 ± 2.9
30.71	75.3 ± 1.6	-1.2	74.1 ± 1.6	74.1 ± 1.6
35.81	30.8 ± 0.7	-1.0	29.8 ± 0.7	29.8 ± 0.7
40.73	8.73 ± 0.5	-0.6	8.13 ± 0.5	8.1 ± 0.5
45.83	1.48 ± 0.19	-0.3	1.18 ± 0.19	1.2 ± 0.2
48.38	0.46 ± 0.12	-0.16	0.30 ± 0.12	0.30 ± 0.12
50.93	0.113 ± 0.038	-0.100	$0.013^{+0.05}_{-0.013}$	$0.01^{+0.05}_{-0.01}$
53.47	0.40 ± 0.09	-0.05	0.35 ± 0.09	0.35 ± 0.04
56.01	0.52 ± 0.10	-0.01	0.51 ± 0.10	0.51 ± 0.10
61.09	1.50 ± 0.18	0	1.50 ± 0.18	1.5 ± 0.2
66.15	1.60 ± 0.18	0	1.60 ± 0.18	1.6 ± 0.2
71.21	0.94 ± 0.14	+0.02	0.96 ± 0.14	0.96 ± 0.14
76.25	0.78 ± 0.12	-0.01	0.77 ± 0.12	0.77 ± 0.12
86.29	0.035 ± 0.025	-0.005	0.030 ± 0.025	0.030 ± 0.025
101.38	0.076 ± 0.034	0	0.076 ± 0.034	0.076 ± 0.034
140.82	0.072 ± 0.028	0	0.072 ± 0.028	0.072 ± 0.028
	±3%		±3%	±4%

total error of scale

Table 1 (continued)

Pion kinetic energy in the lab. system = 200 MeV

Momentum in c.m. system = 300.55 MeV/c

1	2	3	4	5
θ^* (deg)	$\left(\frac{d\sigma}{d\Omega}\right)^*$ (mb/sr)	finite angle correction	$\left(\frac{d\sigma}{d\Omega}\right)^{*FA}$ (mb/sr)	$\left(\frac{d\sigma}{d\Omega}\right)^{*SF}$ (mb/sr)
11.23	459.3 ± 16.4	0	459.3 ± 16.4	480.5 ± 17.3
12.26	421.4 ± 13.1	0	421.4 ± 13.1	441.0 ± 13.9
15.35	356.3 ± 10.8	0	356.3 ± 10.8	372.7 ± 12.9
20.48	225.9 ± 3.6	0	225.9 ± 3.6	236.2 ± 3.9
25.62	129.3 ± 2.7	-1.8	127.5 ± 2.7	133.5 ± 2.9
30.77	59.2 ± 1.8	-1.3	57.9 ± 1.8	60.6 ± 1.9
35.88	21.2 ± 0.7	-1.0	20.2 ± 0.7	21.2 ± 0.8
41.20	4.20 ± 0.31	-0.53	3.67 ± 0.31	3.84 ± 0.33
46.31	0.54 ± 0.11	-0.13	0.41 ± 0.11	0.43 ± 0.12
48.86	0.51 ± 0.10	-0.06	0.45 ± 0.10	0.47 ± 0.10
51.41	0.30 ± 0.08	-0.08	0.22 ± 0.08	0.23 ± 0.08
53.96	0.91 ± 0.12	+0.04	0.95 ± 0.04	0.99 ± 0.13
56.50	1.05 ± 0.10	+0.03	1.08 ± 0.10	1.13 ± 0.10
61.48	1.31 ± 0.14	+0.01	1.32 ± 0.14	1.38 ± 0.15
66.55	1.06 ± 0.13	+0.01	1.07 ± 0.13	1.12 ± 0.14
71.60	0.69 ± 0.18	0	0.69 ± 0.18	0.72 ± 0.19
76.65	0.30 ± 0.04	-0.01	0.29 ± 0.04	0.30 ± 0.04
81.68	0.15 ± 0.02	-0.01	0.14 ± 0.02	0.15 ± 0.02
91.70	0.013 ± 0.006	0	0.013 ± 0.006	0.014 ± 0.006
101.67	0.026 ± 0.008	0	0.026 ± 0.008	0.027 ± 0.008
121.46	0.021 ± 0.006	0	0.021 ± 0.006	0.022 ± 0.006
141.08	0.042 ± 0.029	0	0.042 ± 0.029	0.044 ± 0.030
	±3%		±3%	±4%

total error of scale

Table 1 (continued)

Pion kinetic energy in the lab. system = 230 MeV				
Momentum in c.m. system = 331.42 MeV/c				
1	2	3	4	5
θ^* (deg)	$\left(\frac{d\sigma}{d\Omega}\right)^*$ (mb/sr)	finite angle correction	$\left(\frac{d\sigma}{d\Omega}\right)^{*FA}$ (mb/sr)	$\left(\frac{d\sigma}{d\Omega}\right)^{*SF}$ (mb/sr)
10.42	450.8 ± 16.7	0	450.8 ± 16.7	488.7 ± 18.1
11.46	414.4 ± 15.2	0	414.4 ± 15.2	449.2 ± 16.5
12.49	399.8 ± 12.4	0	399.8 ± 12.4	433.4 ± 13.4
15.58	322.9 ± 9.1	0	322.9 ± 9.1	350.0 ± 9.9
20.74	189.7 ± 4.3	0	189.7 ± 4.3	205.6 ± 4.7
25.90	93.9 ± 2.2	0	93.9 ± 2.2	101.8 ± 2.4
31.03	34.8 ± 1.0	-1.3	33.5 ± 1.0	36.3 ± 1.1
36.19	11.7 ± 0.4	-0.8	10.9 ± 0.4	11.8 ± 0.4
41.20	1.89 ± 0.16	-0.32	1.57 ± 0.16	1.71 ± 0.17
43.76	1.07 ± 0.15	-0.13	0.94 ± 0.15	1.02 ± 0.16
46.32	0.77 ± 0.09	-0.04	0.73 ± 0.09	0.79 ± 0.10
48.87	1.04 ± 0.15	-0.03	1.01 ± 0.15	1.09 ± 0.16
51.42	1.08 ± 0.11	+0.02	1.10 ± 0.11	1.19 ± 0.12
56.52	1.54 ± 0.18	+0.03	1.57 ± 0.18	1.70 ± 0.20
61.61	1.45 ± 0.21	+0.02	1.47 ± 0.21	1.59 ± 0.23
66.68	0.69 ± 0.11	-0.01	0.68 ± 0.11	0.74 ± 0.12
71.74	0.60 ± 0.22	-0.02	0.58 ± 0.22	0.63 ± 0.24
	±3%		±3%	±4%
total error of scale				

Table 1 (continued)

Pion kinetic energy in the lab. system = 260 MeV

Momentum in c.m. system = 361.67 MeV/c

1	2	3	4	5
θ^* (deg)	$\left(\frac{d\sigma}{d\Omega}\right)^*$ (mb/sr)	finite angle correction	$\left(\frac{d\sigma}{d\Omega}\right)^{*FA}$ (mb/sr)	$\left(\frac{d\sigma}{d\Omega}\right)^{*SF}$ (mb/sr)
10.45	522.3 ±46.3	0	522.3 ±46.3	527.5 ±46.8
11.49	445.4 ±26.3	0	445.4 ±26.3	449.9 ±26.6
13.04	450.8 ±23.8	0	450.8 ±23.8	455.3 ±24.0
15.63	303.9 ± 8.6	0	303.9 ± 8.6	306.9 ± 8.7
20.78	183.9 ± 4.4	0	183.9 ± 4.4	185.7 ± 4.4
25.95	83.5 ± 2.0	-3.0	80.5 ± 2.0	81.3 ± 2.0
31.12	30.3 ± 0.9	-1.5	28.8 ± 0.9	29.1 ± 0.9
36.26	8.2 ± 0.5	-0.8	7.4 ± 0.5	7.5 ± 0.5
38.72	4.21± 0.49	-0.53	3.68± 0.49	3.72± 0.49
41.29	1.72± 0.26	-0.31	1.41± 0.26	1.42± 0.26
43.86	1.08± 0.20	-0.13	0.95± 0.20	0.96± 0.20
46.42	1.47± 0.21	+0.03	1.50± 0.21	1.51± 0.21
48.98	1.80± 0.22	+0.08	1.88± 0.22	1.90± 0.22
51.54	1.81± 0.22	+0.03	1.84± 0.22	1.86± 0.22
56.64	1.42± 0.19	+0.01	1.43± 0.19	1.44± 0.19
61.73	1.09± 0.16	0	1.09± 0.16	1.10± 0.16
66.81	0.52± 0.10	-0.01	0.51± 0.10	0.52± 0.10
71.88	0.37± 0.09	-0.01	0.36± 0.09	0.36± 0.09
	±3%		±3%	±4%

total error of scale

Table 1 (continued)

Pion kinetic energy in the lab. system = 280 MeV				
Momentum in c.m. system = 381.60 MeV/c				
1	2	3	4	5
θ^* (deg)	$\left(\frac{d\sigma}{d\Omega}\right)^*$ (mb/sr)	finite angle correction	$\left(\frac{d\sigma}{d\Omega}\right)^{*FA}$ (mb/sr)	$\left(\frac{d\sigma}{d\Omega}\right)^{*SF}$ (mb/sr)
10.99	386.9 ± 14.2	0	386.9 ± 14.2	448.8 ± 16.5
12.55	354.1 ± 12.7	+0.1	354.2 ± 12.7	410.9 ± 14.7
15.13	281.6 ± 9.0	-0.9	280.7 ± 9.0	325.6 ± 10.4
17.72	221.6 ± 6.8	-1.6	220.0 ± 6.8	255.2 ± 7.9
20.31	156.2 ± 4.7	-1.9	154.3 ± 4.7	179.0 ± 5.5
25.49	69.1 ± 2.4	-1.5	67.6 ± 2.4	78.4 ± 2.8
30.64	24.1 ± 1.0	-0.9	23.2 ± 1.0	26.9 ± 1.2
35.81	5.6 ± 0.4	-0.49	5.11 ± 0.4	5.93 ± 0.5
41.46	1.61 ± 0.18	-0.20	1.41 ± 0.18	1.64 ± 0.21
44.03	1.31 ± 0.15	-0.09	1.22 ± 0.15	1.42 ± 0.17
46.59	1.57 ± 0.17	-0.02	1.55 ± 0.17	1.80 ± 0.20
49.15	1.46 ± 0.16	+0.01	1.47 ± 0.16	1.70 ± 0.19
51.71	1.36 ± 0.16	+0.01	1.37 ± 0.16	1.59 ± 0.19
56.82	1.37 ± 0.16	+0.01	1.38 ± 0.16	1.60 ± 0.19
61.92	0.88 ± 0.12	0	0.88 ± 0.12	1.02 ± 0.14
67.00	0.60 ± 0.10	0	0.60 ± 0.10	0.70 ± 0.12
72.07	0.15 ± 0.05	0	0.15 ± 0.05	0.17 ± 0.06
131.09	$\leq$ 0.045		$\leq$ 0.045	$\leq$ 0.052
	±3%		±3%	±7%
total error of scale				

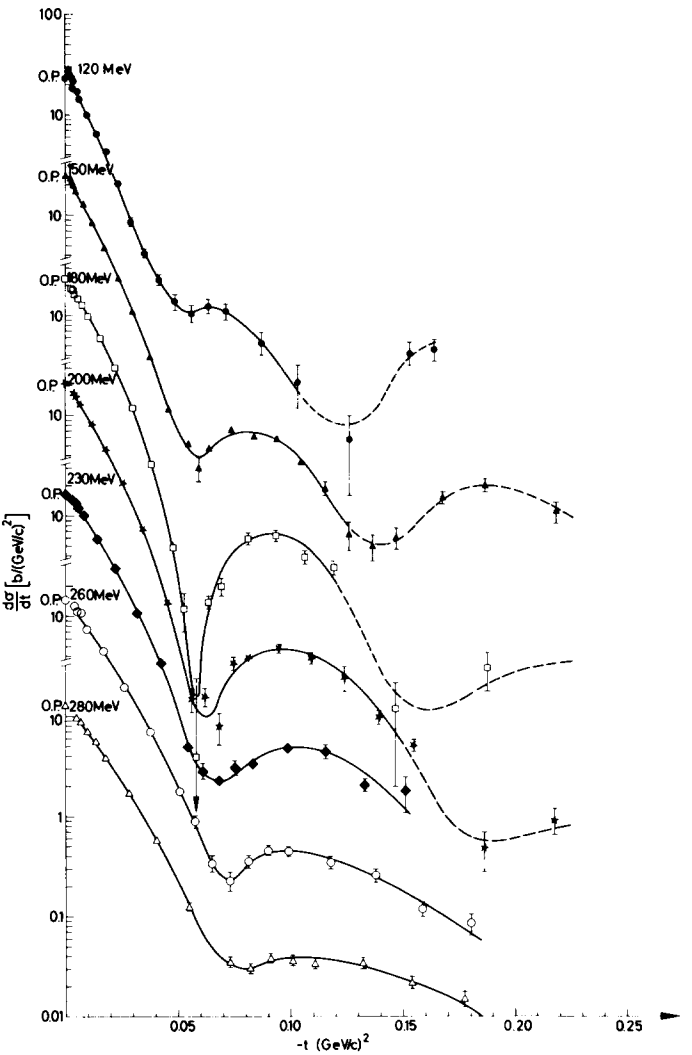

Fig. 3. π^- ^{12}C elastic differential cross sections versus $-t$ squared momentum transfer in the c.m. system, at incident-pion energies of 120, 150, 180, 200, 230, 260 and 280 MeV in the laboratory. The optical point (O. P.) shows the value of $|\mathrm{Im}\, f|^2$ as deduced from our measured total cross sections.

Table 2
Scale factors.

Energy in MeV	120	150	180	200	230	260	280
scale factor	1.04±0.04	0.94±0.05	1.00±0.02	1.047±0.013	1.084±0.012	1.01±0.02	1.16±0.06

a time by the final hodoscope varied from 9 to 18 MeV, depending on the incident momentum and (b) the resolution of the apparatus was sufficient to separate clearly the 4.44 MeV level, the group of levels around 10 MeV (fig. 2) and the $T = 1$ group of levels starting at 15 MeV.

Total cross sections have also been measured by the standard transmission technique. The set-up was placed at the end of the spectrometer, both arms being aligned. Pions were identified with a liquid DISC Čerenkov counter placed just behind the hodoscope (fig. 1) to eliminate contamination bias.

The angular distributions for inelastic scattering covered the same angular and energy ranges as for the elastic ones. Total cross sections were measured in the same energy range, and in addition at 90 and 108 MeV.

The same corrections (apart from the finite angular correction) and error estimations were applied to the inelastic angular distributions as for the elastic distributions. The results are given in table 3 and are represented in fig. 4.

Excitation of the 7.7 MeV level is one or two orders of magnitude smaller than that of the others. It could be measured at only very few angles and for the lowest energies.

Contributions, if any, from the levels at 10.3 and 10.8 MeV could not be subtracted from the 9.6 MeV distribution.

Inelastic scattering through the first isospin 1 levels was only measured between 200 and 280 MeV.

At 260 MeV, the spectrum of inelastic pions having lost up to 100 MeV in the interaction has been measured at angles between 30° and 70°. Individual levels or groups were not identified above 16 MeV excitation. Since this distribution decreases rather rapidly with the excitation energy, one can easily extrapolate it to the higher excitation energies and then integrate the result in order to obtain the inelastic differential cross section given in table 4. The value at 0° is extracted from table 5 (see below).

The results of total cross section measurements are given in table 6 and are shown in fig. 5. Auto-absorption effects in the target have been measured and the consistency of the analysis has been checked by using different thicknesses of carbon between 1 and 4 cm. Extrapolation to 0° was easily made as the elastic differential cross sections had been measured. The results agree rather well with the data of Ignatenko et al. [1]. The 69.5 MeV and 87.5 MeV values of σ_T are deduced from the data of Edelstein et al. [2] by an optical-potential analysis. They agree with an extrapolation of our data.

Table 3
π^- ^{12}C differential inelastic cross section.

Pion kinetic energy in the lab. system in MeV	120		150		180		200		230		260		280	
Momentum in c.m. system in MeV/c	213.92		247.38		279.57		300.55		331.42		361.67		381.60	
	θ^*	$\left(\frac{d\sigma}{d\Omega}\right)^*$	θ^*	$\left(\frac{d\sigma}{d\Omega}\right)^*$	θ^*	$\left(\frac{d\sigma}{d\Omega}\right)^*$	θ^*	$\left(\frac{d\sigma}{d\Omega}\right)^*$	θ^*	$\left(\frac{d\sigma}{d\Omega}\right)^*$	θ^*	$\left(\frac{d\sigma}{d\Omega}\right)^*$	θ^*	$\left(\frac{d\sigma}{d\Omega}\right)^*$
	(deg)	(mb/sr)	(deg)	(mb/sr)	(deg)	(mb/sr)	(deg)	(mb/sr)	(deg)	(mb/sr)	(deg)	(mb/sr)	(deg)	(mb/sr)
	21.05	≤ 6.18	20.50	≤ 4.74	17.88	6.35 ± 6.35	20.59	4.6 ± 3.6	20.54	$1.67^{+2.55}_{-1.67}$	20.79	≤ 3.06	17.74	≤ 4.92
	26.16	≤ 2.79	25.62	4.8 ± 1.4	20.46	≤ 3.6	25.73	6.3 ± 1.2	25.69	9.0 ± 0.9	25.95	4.69 ± 1.43	20.32	≤ 3.21
	31.36	1.19 ± 1.13	30.74	2.8 ± 0.6	25.49	5.7 ± 1.9	30.86	5.7 ± 0.6	30.83	5.4 ± 0.4	31.1	4.92 ± 0.54	25.99	7.9 ± 1.4
	36.46	1.30 ± 0.47	35.85	3.5 ± 0.3	30.61	3.2 ± 0.6	35.99	3.6 ± 0.3	36.07	4.32 ± 0.15	36.25	3.97 ± 0.32	31.16	6.69 ± 0.57
	41.55	1.46 ± 0.43	40.95	2.6 ± 0.2	35.73	3.6 ± 0.3	41.11	2.9 ± 0.3	41.20	3.13 ± 0.19	38.73	2.74 ± 0.41	36.31	3.96 ± 0.33
	46.64	2.20 ± 0.52	46.04	2.22 ± 0.14	40.74	2.1 ± 0.3	46.21	1.92 ± 0.12	43.76	2.48 ± 0.23	41.29	3.24 ± 0.36	41.46	2.72 ± 0.26
	51.72	1.29 ± 0.28	51.13	1.32 ± 0.10	45.85	2.1 ± 0.2	48.77	1.45 ± 0.13	46.32	2.15 ± 0.15	43.86	2.16 ± 0.28	44.02	1.89 ± 0.21
	56.78	0.64 ± 0.19	56.20	0.91 ± 0.06	48.39	1.3 ± 0.2	51.31	1.01 ± 0.08	48.87	1.56 ± 0.18	46.42	1.67 ± 0.22	46.59	1.27 ± 0.17
	61.85	0.67 ± 0.21	58.74	0.72 ± 0.06	50.94	1.12 ± 0.12	53.86	0.94 ± 0.12	51.43	0.85 ± 0.10	48.98	0.83 ± 0.15	49.15	0.90 ± 0.13
	66.90	0.20 ± 0.12	61.273	0.31 ± 0.06	53.48	0.81 ± 0.14	56.40	0.50 ± 0.05	56.52	0.68 ± 0.13	51.54	0.64 ± 0.13	51.71	0.81 ± 0.13
4.43 MeV	71.94	0.12 ± 0.09	66.33	0.16 ± 0.05	56.02	0.37 ± 0.09	61.48	0.15 ± 0.02	61.61	0.16 ± 0.06	56.64	0.44 ± 0.10	56.82	0.45 ± 0.09
	76.98	0.37 ± 0.15	71.38	0.18 ± 0.05	61.10	0.18 ± 0.07	66.55	0.075 ± 0.020	66.68	0.285 ± 0.12	61.74	0.23 ± 0.07	61.92	0.19 ± 0.06
	87.01	0.33 ± 0.13	76.42	0.20 ± 0.05	66.16	$0.020^{+0.03}_{-0.020}$	71.61	0.11 ± 0.02			66.82	0.12 ± 0.08	67.0	0.12 ± 0.05
	97.01	1.16 ± 0.26	81.44	0.36 ± 0.06	71.22	0.06 ± 0.04	76.65	0.089 ± 0.019			72	0.20 ± 0.07	72.1	0.10 ± 0.05
	111.94	0.19 ± 0.14	86.46	0.38 ± 0.05	76.26	0.08 ± 0.05	81.68	0.095 ± 0.016					130.1	≤ 0.049
	131.70	0.38 ± 0.14	91.46	0.37 ± 0.06	86.30	0.15 ± 0.06	91.70	0.067 ± 0.014						
	141.54	0.55 ± 0.15	96.46	0.45 ± 0.05	101.28	0.02 ± 0.02	101.67	0.015 ± 0.006						
			101.44	0.35 ± 0.05	140.72	0.19 ± 0.05	121.47	0.071 ± 0.012						
			111.37	0.35 ± 0.04			141.08	0.071 ± 0.013						
			121.26	0.15 ± 0.04										
			140.93	0.33 ± 0.03										

Table 3 (continued)

7.66 MeV	87.01	0.37 ± 0.15	61.28	0.11 ± 0.06	66.17	0.068	$^{+0.039}_{-0.049}$									
	111.94	0.57 ± 0.20	66.34	0.06 ± 0.05	101.28	0.05	± 0.03									
					139.7	0.04	± 0.03									
			30.74	0.63 ± 0.03	17.89	0.85	± 0.36	30.86	1.99	± 0.70	25.16	2.28	± 0.80	31.11	1.33 ± 0.41	31.16	2.18 ± 0.56
			35.85	0.75 ± 0.21	30.51	0.51	$^{+0.70}_{-0.51}$	35.99	1.33	± 0.17	30.94	1.35	± 0.27	36.26	2.05 ± 0.33	36.31	2.90 ± 0.30
			40.95	0.89 ± 0.17	35.63	1.16	± 0.33	41.11	1.57	± 0.20	36.07	1.82	± 0.15	38.73	1.90 ± 0.37	41.46	2.34 ± 0.24
			46.05	0.93 ± 0.12	40.73	1.49	± 0.22	46.22	1.41	± 0.10	41.20	1.95	± 0.18	41.30	1.61 ± 0.26	44.03	1.53 ± 0.19
			51.13	0.88 ± 0.10	45.85	1.18	± 0.14	48.77	1.35	± 0.12	43.76	1.29	± 0.18	43.86	1.47 ± 0.24	46.60	1.47 ± 0.19
			56.21	0.68 ± 0.06	48.40	0.94	± 0.17	51.32	0.95	± 0.09	46.32	1.23	± 0.12	46.42	1.33 ± 0.21	49.16	1.27 ± 0.17
			58.75	0.48 ± 0.06	50.95	1.10	± 0.12	53.87	0.84	± 0.12	48.88	1.32	± 0.18	48.99	1.47 ± 0.20	51.72	1.01 ± 0.14
			61.28	0.40 ± 0.07	53.49	0.92	± 0.15	56.41	0.70	± 0.07	51.43	0.93	± 0.12	51.54	0.70 ± 0.14	56.83	0.36 ± 0.08
			66.34	0.38 ± 0.06	56.03	0.85	± 0.15	61.49	0.40	± 0.04	56.53	0.59	± 0.12	56.65	0.45 ± 0.11	61.92	0.29 ± 0.07
9.64 MeV			71.39	0.18 ± 0.05	61.31	0.49	± 0.11	66.56	0.20	± 0.03	61.61	0.19	± 0.07	61.74	0.24 ± 0.08	67.00	0.11 ± 0.05
			76.43	0.16 ± 0.05	66.17	0.068	± 0.05	71.61	0.099	± 0.022				66.82	0.29 ± 0.10	72.10	0.03 ± 0.02
			81.45	0.17 ± 0.05	71.22	0.11	± 0.05	76.66	0.070	± 0.017						131.68	⩽ 0.06
			86.47	0.28 ± 0.05	76.26	0.19	± 0.07	81.69	0.084	± 0.017							
			91.47	0.32 ± 0.07	87.71	0.08	± 0.05	91.71	0.081	± 0.016							
			96.47	0.34 ± 0.05	101.29	0.14	± 0.05	101.68	0.049	± 0.012							
			101.45	0.37 ± 0.05				121.47	0.069	± 0.014							
			111.38	0.34 ± 0.04				141.09	0.092	± 0.015							
			121.27	0.29 ± 0.04													
			140.94	0.23 ± 0.04													
								35.99	0.76	± 0.27	36.10	0.88	± 0.25	38.41	0.85 ± 0.35	31.16	3.18 ± 0.75
								46.22	0.51	± 0.08	41.21	0.42	± 0.42	40.96	0.57 ± 0.27	36.32	1.60 ± 0.51
								48.78	0.46	± 0.13	46.33	0.85	± 0.15	43.51	0.49 ± 0.24	41.46	0.97 ± 0.19
								51.33	0.41	± 0.06	51.44	0.40	± 0.15	66.35	0.17 ± 0.10	44.03	0.78 ± 0.15
$T = 1$								53.87	0.39	± 0.07						46.60	0.45 ± 0.11
≈ 15.1 MeV								56.42	0.32	± 0.07						49.16	0.59 ± 0.12
								61.50	0.18	± 0.04						51.72	0.57 ± 0.11
								66.56	0.11	± 0.03						56.83	0.37 ± 0.09
								101.69	0.038	± 0.012						61.93	0.21 ± 0.08
								141.09	0.105	± 0.018						67.01	0.17 ± 0.08

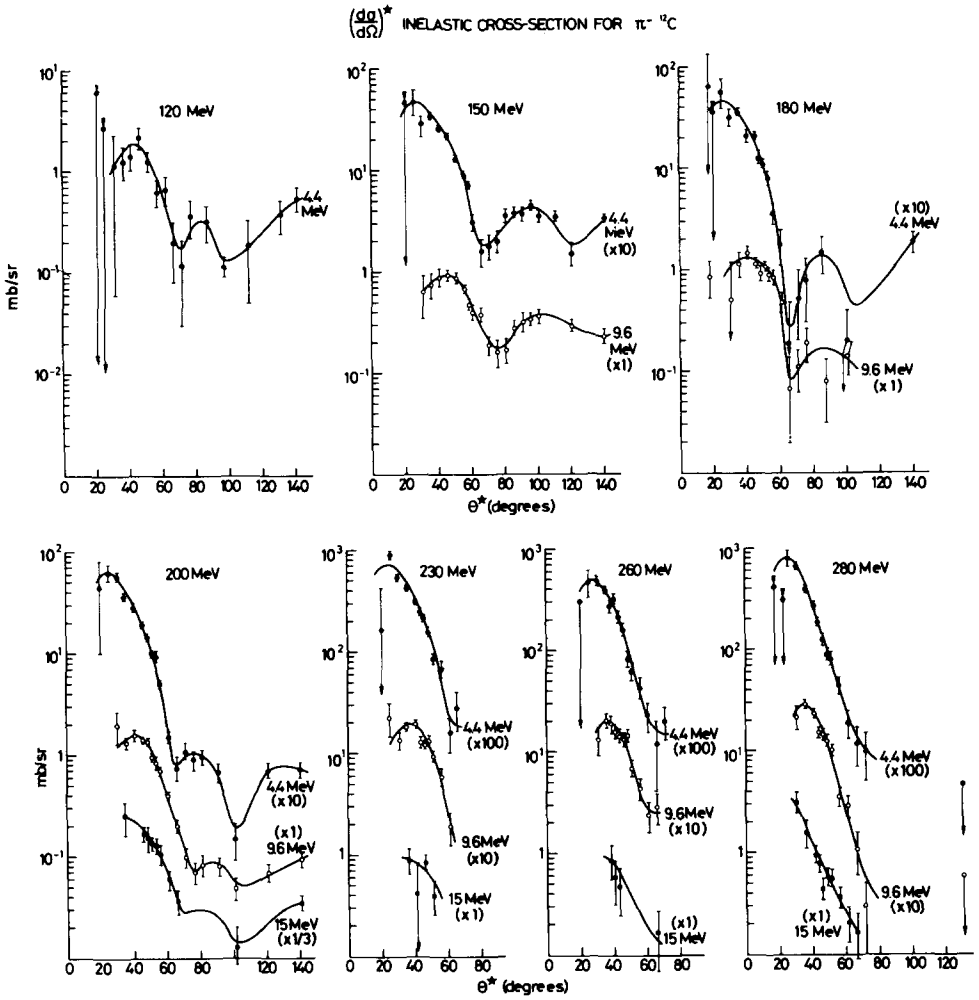

Fig. 4. Inelastic reactions $\pi^- + {}^{12}C \rightarrow \pi^- + {}^{12}C^*$. Excitation differential cross sections versus the scattering angle in the c.m. system θ^* at incident-pion energies of 120, 150, 180, 200, 230, 260, 280 MeV and for: (a) the first excited state of ^{12}C at 4.43 MeV; (b) the group of levels around 10 MeV (9.64, 10.3 and 10.8 MeV levels); (c) the first $T = 1$ levels near 15 MeV (15.1, 16.1, 16.6 and 17.2 MeV levels).

In order to separate more clearly the excitation curves, they have been multiplied by a factor indicated between brackets. To obtain the true values of the cross sections one has thus to divide by this factor the value read on the scale.

Table 4
Inelastic differential cross section at 260 MeV.

Angles in degrees	$d\sigma/d\Omega$ inelastic total ($mb \cdot sr^{-1}$)
0	49 ± 5
30	30 ± 5
40	19 ± 4
50	13 ± 5
60	8 ± 2
70	5.3 ± 2.5

Table 5
Total inelastic cross section at 0 degree.

Energy (MeV)	$(d\sigma/d\Omega)$ 0^{o} total inelastic (mb/sr)
108	115.2 ± 14.4
120	68.6 ± 10.6
150	16.0 ± 4.8
180	22.2 ± 4.8
200	31.6 ± 5.2
230	46.0 ± 5.2
260	49.1 ± 5.4
280	77.0 ± 8.4

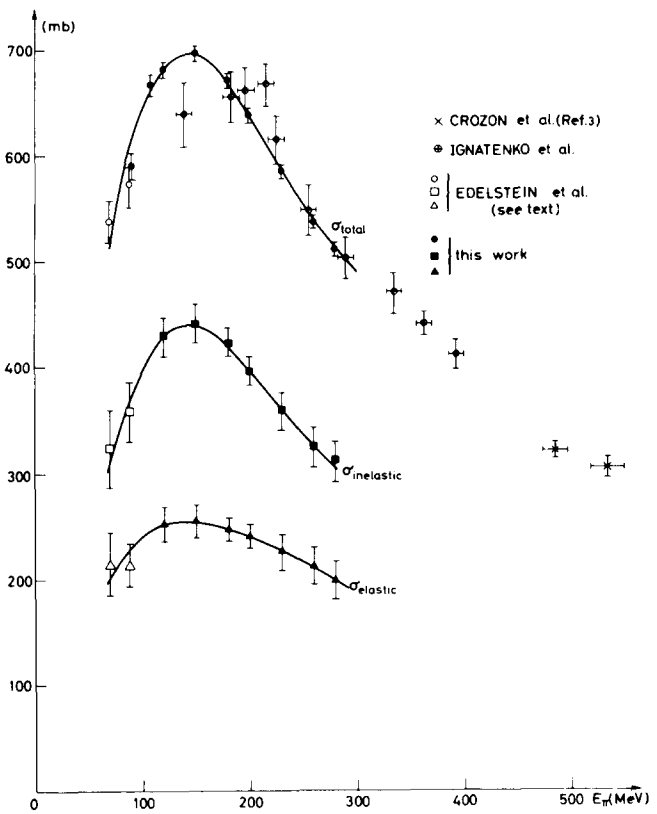

Fig. 5. π^{-} ^{12}C total cross section, total elastic cross section, and total inelastic cross section versus the π^{-} energy in the laboratory. The values of the total cross section at 69.5 MeV and 87.5 MeV are deduced by an optical-potential analysis of the data obtained by Edelstein et al.

Table 6
π^- ^{12}C elastic, inelastic and total cross sections.

Energy (MeV)	σ_{total} (mb)	σ_{el} (mb)	σ_{inel} (mb)	$\sigma_{el}/\sigma_{inel}$
69.5 *	537 ± 20	214 ± 30	323 ± 36	0.663 ± 0.119
87.5 *	571 ± 20	213 ± 20	358 ± 28	0.595 ± 0.073
90	590 ± 12			
108	666 ± 10			
120	681 ± 7	252 ± 16	429 ± 18	0.587 ± 0.045
150	696 ± 7	255 ± 16	441 ± 18	0.578 ± 0.043
180	670 ± 7	247 ± 11	423 ± 13	0.584 ± 0.032
200	637 ± 7	241 ± 11	396 ± 13	0.609 ± 0.034
230	584 ± 6	225 ± 17	359 ± 18	0.626 ± 0.053
260	536 ± 6	212 ± 18	324 ± 19	0.654 ± 0.068
280	510 ± 6	199 ± 18	311 ± 19	0.640 ± 0.070

* Ref. [3]

As a by-product of these measurements, the differential cross section at 0^o for inelastic pions (i.e. all reactions, except elastic scattering, in which the pion is re-emitted) has been deduced (table 5 and fig. 6).

From the elastic differential cross section and total cross section data, total elastic and total inelastic cross sections have been evaluated. They are also given in table 6 and shown in fig. 5.

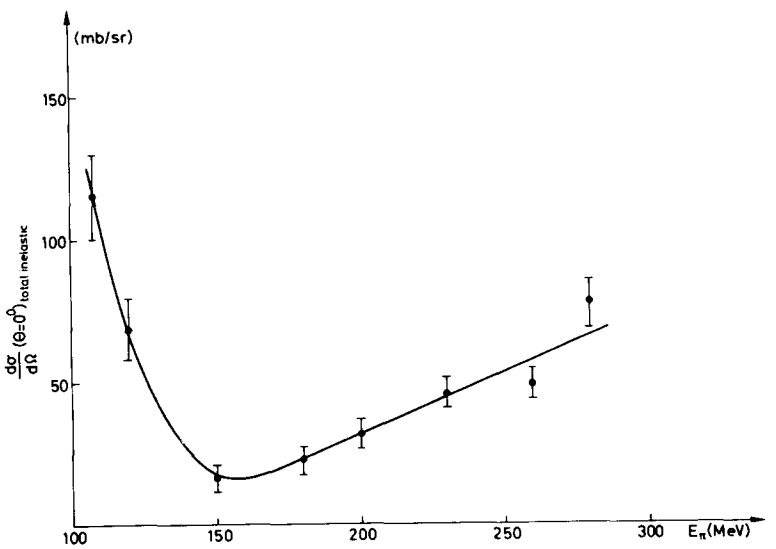

Fig. 6. Inelastic reaction $\pi^- + {}^{12}C \rightarrow \pi^- + {}^{12}C^*$. Differential cross section at 0^o, integrated over all inelastic channels, as a function of the pion energy in the laboratory.

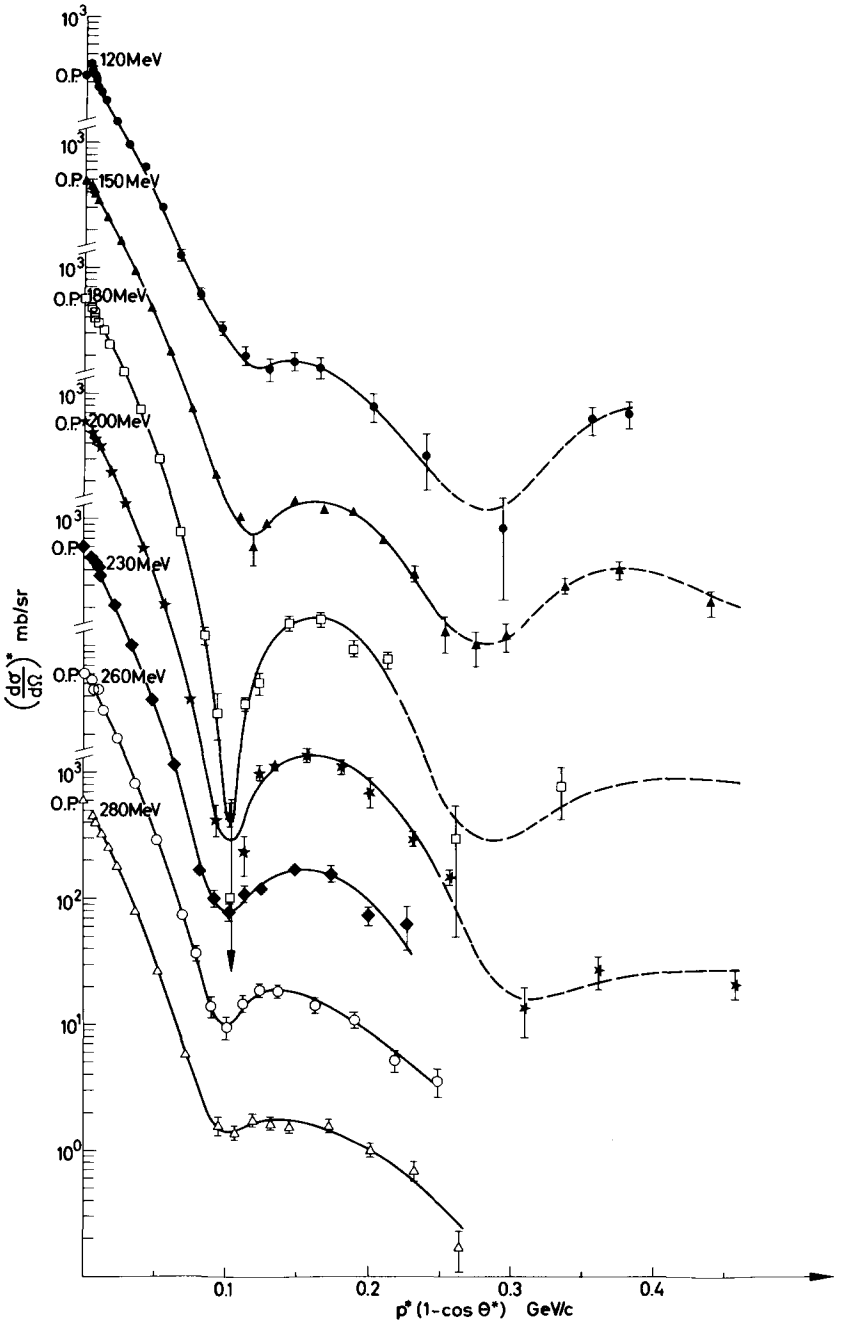

Fig. 7. π^- ^{12}C elastic differential cross sections as a function of p^* $(1-\cos\theta^*)$, longitudinal momentum transfer in the c. m. system, at incident pion energies of 120, 150, 180, 200, 230, 260 and 280 MeV.

5. DISCUSSION OF THE RESULTS

The elastic scattering data show a marked variation around 180 MeV. This is probably due to the influence of the $(\frac{3}{2}, \frac{3}{2})$ pion-nucleon resonance. The maximum depth of the first minimum in the elastic-scattering angular distribution occurs at 180 MeV. The depth varies by a large factor around this value. Moreover, if one represents these data versus the longitudinal momentum transfer (fig. 7), the position of the first minimum and of the first maximum remains rather constant against incident pion energy. Particularly, the first minimum occurs at a value of about 100 MeV/c longitudinal momentum transfer.

The total cross section has a maximum at 145 ± 8 MeV, like the total elastic and the total inelastic ones. This value is low compared to the energy of the first pion-nucleon resonance, even if one takes into account the kinematical effect due to the mass of ^{12}C.

In the range of our measurements, the total elastic scattering is always of the order of 0.6 of the inelastic one. This indicates that the nucleus is not totally absorbing for pions, even at the pion-nucleon resonance.

The differential cross section at 0^o for inelastic pions is very large, of the order of 110 mb/sr at 110 MeV, goes to a minimum of 15 mb/sr at 155 MeV, and then slowly rises again to reach 70 mb/sr at 280 MeV. The large value at 110 MeV implies of course a large forward peaking. At 155 MeV, its very low value is compatible with a more isotropic distribution and/or absorption of the pions. It is also known from our measurements that the differential cross section at 260 MeV for all inelastic pions is a distribution that has a maximum at 0^o and a half-width of 35^o to 40^o. The mean transverse momentum of the inelastic pion spectrum is about 230 MeV/c, i.e. of the same order of magnitude as that of the Fermi motion.

These facts suggest the following qualitative picture: (a) Around 110 MeV, the strong nuclear excitation when pions are re-emitted is largely peripheral. (b) Around 155 MeV, the influence of the πN resonance either leads to a more isotropic distribution of the re-emitted pions, or to strong absorption, or both. This isotropic distribution could be explained if one supposes an intermediate compound system in which, either a nucleon of the nucleus is transformed into a N^*, or some resonant π-nucleus system is formed. (c) At larger energies, as its wavelength gets smaller, the pion may enter more deeply into the nucleus, may suffer more than one scattering on the individual nucleons, and be re-emitted with a transverse momentum distribution near to that of Fermi momentum.

The differential cross sections for the excitation of the first $T = 1$ levels around 15 MeV are of the same order of magnitude as those for the $T = 0$ levels, in agreement with the fact that $T = 1$ pions may induce $\Delta T = 0$, 1 or 2 transitions.

We thank the MSC Division for its support which made it possible to build the variable-energy pion beam. We are especially grateful to Professor P. Preiswerk and Dr. T. E. O. Ericson for their continuous interest in this work. Professor M. Jean was one of the initiators of the experiment.

We wish to thank him for much advice and encouragement. Thanks are due to Mr. R. Meunier who took part in the development of this experiment and participated in a large part of the data taking. We are pleased to acknowledge stimulating discussions with Dr. M. Krell, Dr. M. P. Locher and Professors F. Becker and P. Huguenin. Thanks are due to Dr. J. Renuart for his help in the course of data handling. We are indebted to Dr. A. J. Herz for kind criticism of the manuscript.

Remark: In the figures all data curves are hand drawn and serve mainly to guide the eye.

REFERENCES

[1] A. E. Ignatenko, Proc. CERN symposium (CERN, Geneva, 1956) vol. 2, p. 313.
[2] R. M. Edelstein, W. F. Baker and J. Rainwater, Phys. Rev. 122 (1961) 252.
[3] M. Crozon, Ph. Chavanon, A. Courau, Th. Leray, J. L. Narjoux and J. Tocqueville, Nucl. Phys. 64 (1965) 567.